17th Australasian Fluid Mechanics Conference
Auckland, New Zealand
5-9 December 2010

The influence of pipe length in direct numerical simulation

C. Chin[1], A. Ooi[1], I. Marusic[1] and H. M. Blackburn[2]

[1]Department of Mechanical Engineering
University of Melbourne, Victoria 3010, Australia

[2]Department of Mechanical and Aerospace Engineering
Monash University, Victoria 3186, Australia

Abstract

A direct numerical simulation (DNS) of fully developed turbulent pipe flow is performed at $Re_\tau \approx 170$ and 500 to examine the effect of the streamwise domain length on the convergence of turbulence statistics. Computational domain lengths vary from the $\pi\delta$ to $20\pi\delta$. Lower order statistics such as mean flow, turbulence intensities, Reynolds stress, correlations and higher order statistics including energy spectra, skewness and flatness were computed. The findings show that in the near wall region (below the buffer region, $r^+ \leq 30$), the required pipe length for all turbulence statistics to converge requires a minimum viscous length of $O(6300)$ wall units. It was also found that for convergence of turbulence statistics at the outer region, a proposed pipe length of $8\pi\delta$ seems sufficient for the Reynolds numbers considered in this study.

Introduction

The vast amount of data that can be obtained from DNS has enabled scientists to better understand turbulent flow physics and is becoming an important tool in turbulence research [17]. One of the pioneering study using DNS is that of a three-dimensional isotropic turbulence by Orszag & Patterson [21]. The advancement in computer technology has led to more DNS studies being carried out on turbulent wall-bounded flows, see figure 1. With Reynolds numbers of DNS approaching nominally similar Reynolds numbers as experiments, it is therefore possible to compare turbulence statistics between them. However, early hot-wire experiments have shown that long streamwise structures exist in wall-bounded turbulent flows [9, 24], and recent experiments by Kim & Adrian [16] have shown from premultiplied spectra that these structures were longer than previously appreciated. Balakumar & Adrian [4] termed these structures as "large-scale motions" (LSMs) as motions with wavelength of up to 2-3δ, where δ is the half channel height, pipe radius or boundary later thickness and "very-large-scale motions" (termed VLSMs with wavelength of more than 3δ). A recent study by Hutchins & Marusic [11] reported long meandering features exceeding 20δ in the logarithmic region of turbulent boundary layers, and termed them as "superstructures". Other reports by Monty *et al*. [19, 18] showed that these long meandering features in pipe and channel are up to 25δ in length. Therefore, it is important to better understand how statistics are influenced by how the boundary conditions interact with the largest scale motion in DNS, since its impractical to have a computational domain of infinite length. In this paper, we will investigate the length of domain required in order to obtain converged statistics and the effects of computational domain length on turbulence statistics. The Reynolds numbers chosen for this study are $Re_\tau \approx 170$ and 500.

Discretisation

The numerical scheme employed in this study is detailed in Blackburn & Sherwin [5]. The scheme uses a spectral element discretisation in the meridional semi-plane with a 10^{th} order Gauss-Lobatto-Legendre nodal-based expansion in each element and a Fourier discretisation in the azimuthal direction. The axial, radial and azimuthal directions are denoted as x, r, and θ and N_x, N_r and N_θ are the number of elements. The axial, radial and azimuthal velocities are denoted by U_x, U_r and U_θ with the corresponding fluctuating components as u, u_r and u_θ respectively. A periodic boundary condition is specified in the axial direction. The details of the computational domains for both Reynolds numbers are summarized in table 1, here the '+' symbol denotes scaling with viscous units ν/u_τ, where u_τ is the friction velocity and *nu* is the viscosity. The spatial resolutions

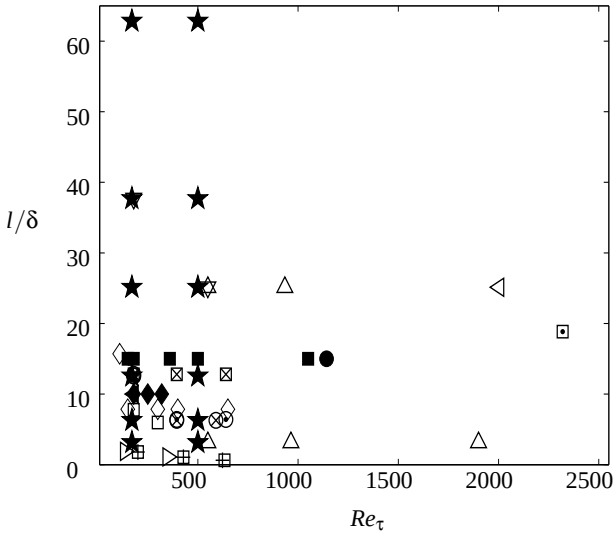

Channel flow DNS		Pipe flow DNS	
Kim *et al*. [15]	◯	Satake *et al*.[22]	■
Jiménez & Pinelli [14]	⊞	Eggels *et al*. [8]	◀
Abe *et al*.[2]	⊙	Wagner *et al*. [25]	♦
Abe *et al*.[1]	⊠	Wu & Moin [26]	●
Antonia *et al*. [3]	□	**Current Study**	★
Moser *et al*. [20]	⊗		
del Álamo & Jiménez [6]	▽		
Iwamoto *et al*. [13]	◊		
del Álamo *et al*. [7]	△		
Iwamoto *et al*. [12]	⊡		
Toh & Itano [23]	▷		
Hoyas & Jiménez [10]	◁		

Figure 1: Previous wall-bounded DNS studies for pipe and channel.

Re_τ	170	500
Pipe Length (L_x)	[πδ, 2πδ, 4πδ, 8πδ, 12πδ, 20πδ]	[πδ , 2πδ, 4πδ, 8πδ, 12πδ, 20πδ]
Symbol	[−− , ◯ , + , □ , ▽ , ×]	[−− , ◯ , + , □ , ▽ , ×]
N_x	[8, 16, 32, 64, 96, 160]	[23, 46, 92, 194, 276, 460]
N_r	8	16
N_θ	128	384
Δx^+	6.7	6.8
Δr^+	[0.5, 3.6]	[0.07, 5.5]
$\Delta r\theta^+$ (at wall)	8.4	8.2

Table 1: Summary of numerical simulation parameters.

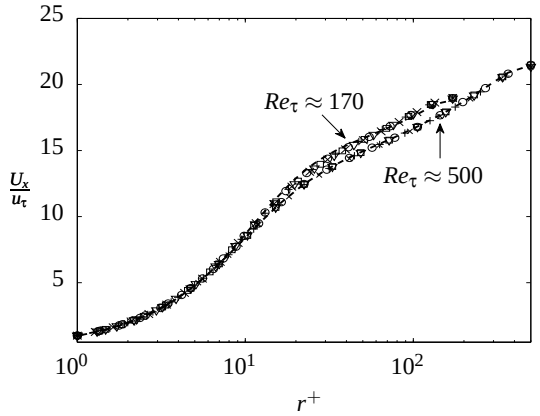

Figure 2: Mean Velocity profiles for $Re_\tau \approx 170$ and 500 for different pipe lengths. Symbols are as in table 1.

for different domains are kept constant for each Reynolds number. This ensures that effects on turbulence statistics is purely due to domain length variation and is not influenced by spatial resolution issues.

Results

The mean velocity profiles for both Reynolds numbers are shown in figure 2. Here we show the velocity profiles for all pipe lengths as a function of normalized wall-normal direction, where $r^+ = 0$ is the wall. It can be seen that the only profile that does not converge is that of $Re_\tau \approx 170$ at pipe length of πδ.

In figure 3, the turbulence intensities for different pipe lengths are shown. For $Re_\tau \approx 170$, pipe lengths of πδ and 2πδ fail to converge. The huge increase in the peak intensity (at $r^+ = 15$, shown as dotted line) for πδ is mainly due to artificial large structures in the flow as will be discussed later. For $Re_\tau \approx 500$, a minimum pipe length of 2πδ seems sufficient for statistics to converge. We have plotted the Reynolds stress $-\overline{u'u'_r}^+$ in figure 4. The results show that the profile at $Re_\tau \approx 170$ at $L_x = \pi\delta$ fails to converge. Even though the order of statistics for both Reynolds stress and turbulence intensity are the same, the radial velocity components are less affected by pipe length and hence the finding is similar to that of the mean velocity profile. Next we show the cross-correlation between axial fluctuating wall shear stress τ_x and axial fluctuating velocity u. Figure 5 show the contours of correlation coefficient as a function of r^+ and axial separation distance Δx^+ for different pipe lengths, outermost contour begins at 0.05 with increment of 0.25. Contour lines for, $L_x = \pi\delta, 2\pi\delta$ for $Re_\tau \approx 170$ and $L_x = \pi\delta, 2\pi\delta$ for $Re_\tau \approx 500$, that do not close, suggest 'contamination' of structures in the flow (in an average sense) owing to the periodicity

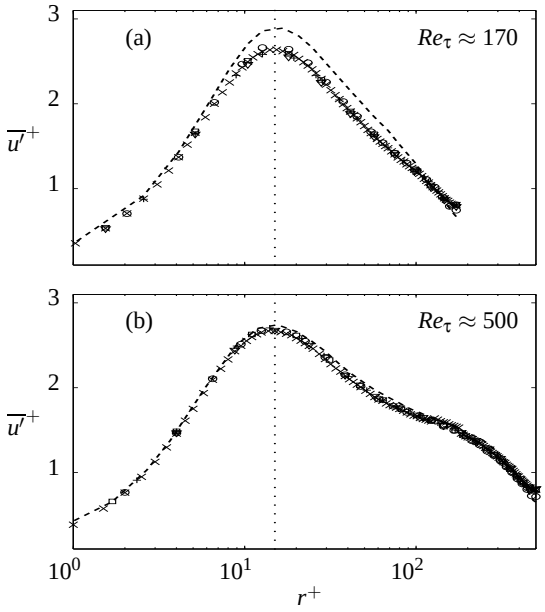

Figure 3: Streamwise turbulence intensity for different pipe length. (a) $Re_\tau \approx 170$, (b) $Re_\tau \approx 500$. The dotted lines are at $r^+ = 15$. Symbols are as in table 1.

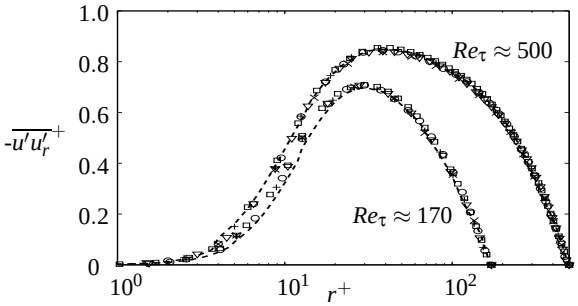

Figure 4: Reynolds stress $-\overline{u'u'_r}^+$ for different pipe lengths at $Re_\tau \approx 170$ and 500. Symbols are as in table 1.

in the streamwise direction. This is due to having pipe lengths that are too short to accommodate the longest structures in the flow field. This translates to having infinitely long structures constantly having an influence on the wall shear stress. It would seem that these 'infinite long structures' contribute to the higher peak turbulence intensity as seen in figure 3. In figure 6, the premultipled one-dimensional energy spectra is plotted as a function of r^+ and streamwise wavelength λ_x^+. We have chosen the four longest pipe lengths ($L_x = 4\pi\delta$(dot-dashed line ▬·▬·▬), 8πδ(dotted line ⋯), 12πδ(dashed-line −−) & 20πδ(solid line

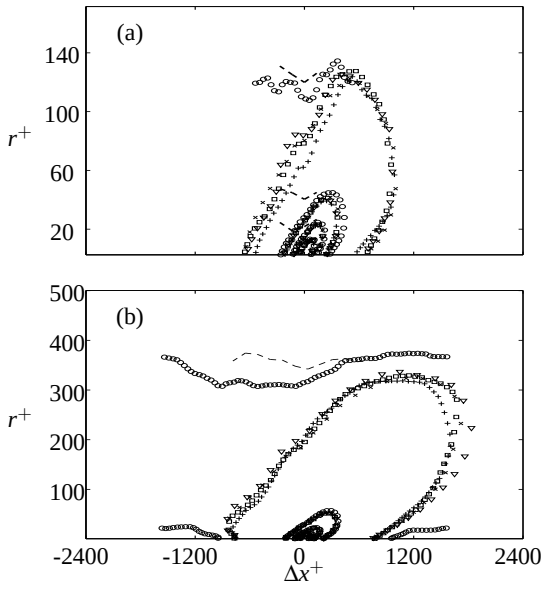

Figure 5: Cross correlation of τ_x and u for different pipe lengths at (a) $Re_\tau \approx 170$ and (b) $Re_\tau \approx 500$. Symbols are as in table 1. Contour lines begin at 0.05 (outermost) with increment of 0.25.

———)) to illustrate the effect of insufficient pipe length on the energy spectra. These pipe lengths are chosen because earlier computed lower order statistics show a minimum length of $4\pi\delta$ for convergence. Results for both Reynolds numbers seem to suggest a pipe length of $8\pi\delta$ for statistics to achieve convergence. The skewness for axial fluctuating velocity u in the near-wall region is shown in figure 7. It is apparent at $Re_\tau \approx 170$, results do not converge for pipe lengths less than $4\pi\delta$. Whereas the results for $Re_\tau \approx 500$ seems to show convergence for all pipe lengths in the near-wall. Similar results are found for flatness for axial fluctuating velocity u as shown in figure 8.

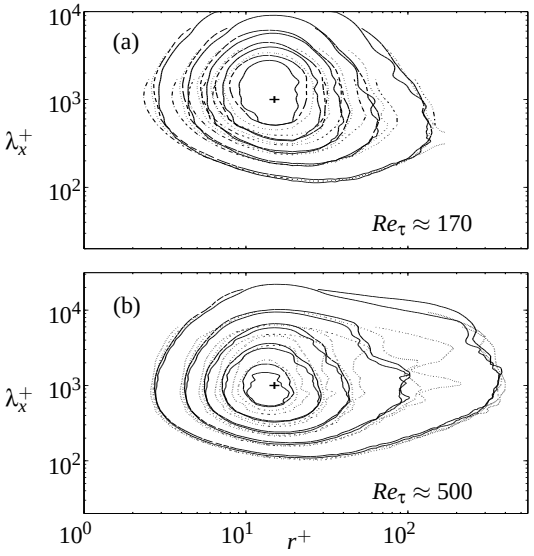

Figure 6: Pre-multiplied energy spectra for streamwise velocity u for (a) $Re_\tau \approx 170$ and (b) $Re_\tau \approx 500$ for all wall normal locations r^+. Contour lines are from 0.35 (outermost) with increment of 0.4. The symbols used are $4\pi\delta$ (dot-dashed line - · — · -), $8\pi\delta$ (dotted line ·····), $12\pi\delta$ (dashed-line – –) and $20\pi\delta$ (solid line ———). The (+) symbol is at $r^+ \approx 15$ and $\lambda_x^+ \approx 1000$.

Conclusions

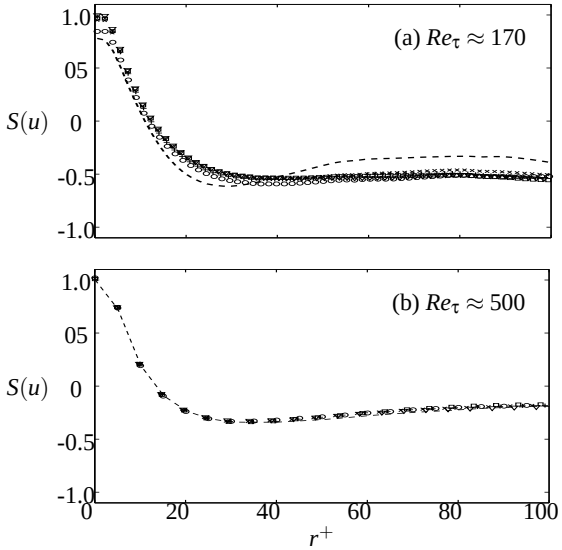

Figure 7: Skewness $S(u) = \overline{u^3}/\overline{u^2}^{3/2}$ for different pipe lengths at (a) $Re_\tau \approx 170$ and (b) $Re_\tau \approx 500$. Symbols are as in table 1.

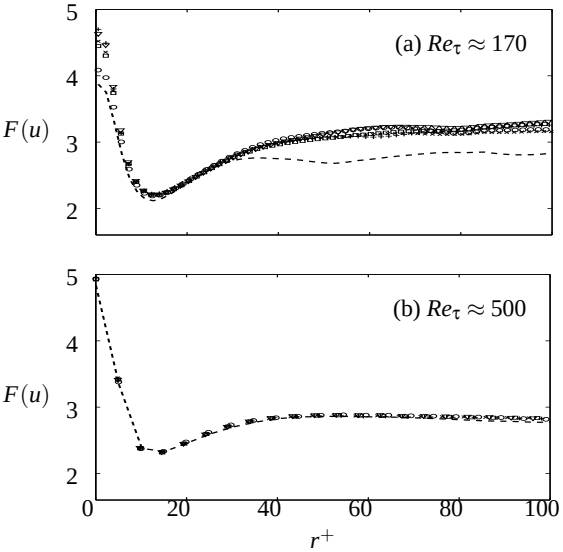

Figure 8: Flatness $F(u) = \overline{u^4}/\overline{u^2}^2$ for different pipe lengths at (a) $Re_\tau \approx 170$ and (b) $Re_\tau \approx 500$. Symbols are as in table 1.

The influence of varying the computational pipe length on turbulence statistics were investigated. The results are summarized in table 2. Findings show that different statistics require different pipe lengths for convergence. To obtain converged results in the near-wall region, a pipe length scaled in viscous units of $L_x^+ \approx O(6300)$ seems sufficient. For most statistics to achieve convergence, a recommended pipe length of $L_x \approx 8\pi\delta$ seems sufficient.

Acknowledgements

We would like to gratefully acknowledge the financial support of the Australian Research Council and APAC's Merit Allocation Scheme and VPAC for the computational resources.

References

[1] Abe, H., Kawamura, H. and Choi, H., Very large-scale structures and their effects on the wall shear-stress fluctuations in a turbulent channel flow up to Re_τ = 640, *Journal*

Turbulence Statistics	*Min length* (δ)		*Min length* ($^+$)	
	$Re_\tau = 170$	$Re_\tau = 500$	$Re_\tau = 170$	$Re_\tau = 500$
Mean velocity profile	2π	π	1000	1500
Turbulence intensity	4π	2π	2100	3100
Reynolds stress	2π	π	1000	1500
Cross-Correlations	8π	4π	4300	6300
1d energy spectra	8π	8π	4300	12300
Skewness, $r^+ < 100$	4π	π	2100	1500
Flatness, $r^+ < 100$	4π	π	2100	1500

Table 2: Table of summary for estimated minimum computational pipe length for convergence of different turbulence statistics for both $Re_\tau \approx 170$ and 500. The second column displays minimum length in terms of pipe radius (δ) and the last column is in terms of viscous length scale ($^+$).

of Fluids Engineering, **126**, 2004, 835 – 843.

[2] Abe, H., Kawamura, H. and Matsuo, Y., Direct numerical simulation of a fully developed turbulent channel flow with respect to the Reynolds number dependence, *Journal of Fluids Engineering*, **123**, 2001, 382 – 393.

[3] Antonia, R., Teitel, M., Kim, J. and Browne, L. W. B., Low-Reynolds-number effects in a fully developed turbulent channel flow, *Journal of Fluid Mechanics.*, **236**, 1992, 579 – 605.

[4] Balakumar, B. J. and Adrain, R. J., Large-and very-large-scale motions in channel and boundary-lyer flows, *Phil. Trans. R. Soc. A.*, **365**, 2007, 665–681.

[5] Blackburn, H. M. and Sherwin, S. J., Formulation of a Galerkin spectral element-Fourier method for three-dimensional incompressible flows in cylindrical geometries, *Journal of Computational Physics*, **197**, 2004, 759 – 778.

[6] del Álamo, J. C. and Jiménez, J., Spectra of the very large anisotropic scales in turbulent channels, *Physics of Fluids.*, **15**, 2003, L41 – L44.

[7] del Álamo, J. C., Jiménez, J., Zandonade, P. and Moser, R. D., Scaling of the energy spectra of turbulent channels, *Journal of Fluid Mechanics.*, **500**, 2004, 135 – 144.

[8] Eggels, J. G. M., Unger, F., Weiss, M. H., Westerweel, J., Adrian, R. J., Friedrich, R. and Nieuwstadt, F. T. M., Fully developed turbulent pipe flow: a comparison between direct numerical simulation and experiment, *Journal of Fluid Mechanics.*, **268**, 1994, 175 – 209.

[9] Favre, A. J., Gaviglio, J. J. and Dumas, R. J., Space-time double correlations and spectra in a turbulent boundary layer, *Journal of Fluid Mechanics.*, **2**, 1957, 313–342.

[10] Hoyas, S. and Jiménez, J., Scaling of the velocity fluctuations in turbulent channels up to Re_τ = 2003, *Physics of Fluids*, **18**, 2006, (011702).

[11] Hutchins, N. and Marusic, I., Evidence of very long meandering features in the logarithmic region of turbulent boundary layers, *Journal of Fluid Mechanics.*, **579**, 2007, 1–28.

[12] Iwamoto, K., Kasagi, N. and Suzuki, Y., Direct numerical simulation of turbulent channel flow at Re_τ = 2320, in *Proc. 6th Symp. Smart Control of Turbulence*, 2005, 327–333, 327–333.

[13] Iwamoto, K., Suzuki, Y. and Kasagi, N., Reynolds number effect on wall turbulence: toward effective feedback control, *Int. J. Heat Fluid Flow*, **23**, 2002, 678 – 689.

[14] Jiménez, J. and Pinelli, A., Autonomous cycle of near-wall turbulence, *Journal of Fluid Mechanics.*, **389**, 1999, 335 – 359.

[15] Kim, J., Moin, P. and Moser, R., Turbulence statistics in fully developed channel flow at low Reynolds number, *Journal of Fluid Mechanics.*, **177**, 1987, 133 – 166.

[16] Kim, K. C. and Adrian, R. J., Very large-scale motion in the outer layer, *Physics of Fluids.*, **11**(2), 1999, 417–422.

[17] Moin, P. and Mahesh, K., Direct numerical simlation: A tool in turbulence research, *Annu. Rev. Fluid Mech.*, **30**, 1998, 539 – 578.

[18] Monty, J. P., Hutchins, N., Ng, H. C. H., Marusic, I. and Chong, M. S., A comparison of turblent pipe, channel and boundary layer flows, *Journal of Fluid Mechanics.*, **632**, 2009, 431 – 442.

[19] Monty, J. P., Stewart, J. A., Williams, R. C. and Chong, M. S., Large-scale features in turbulent pipe and channel flows, *Journal of Fluid Mechanics.*, **589**, 2007, 147 – 156.

[20] Moser, R. D., Kim, J. and Mansour, N. N., Direct numerical simulation of turbulent channel flow up to Re_τ = 590, *Physics of Fluids*, **11,4**, 1999, 943 – 945.

[21] Orszag, S. A. and Patterson, G. S., Numerical simulation of three-dimensional homogeneous isotropic turbulence, *Physical Review Letters*, **28**, 1972, 76 – 79.

[22] Satake, S., Kunugi, T. and Himeno, R., High Reynolds number computation for turbulent heat transfer in a pipe flow, in *Lecture Notes in Computer Science*, Springer Berlin / Heidelberg, 2000, 514 – 523, 514 – 523.

[23] Toh, S. and Itano, T., Interaction between a large-scale structure and near-wall structures in channel flow, *Journal of Fluid Mechanics.*, **524**, 2005, 249 – 262.

[24] Townsend, A. A., *The Structure of Turbulent Shear Flow*, Cambridge University Press, 1956.

[25] Wagner, C., Hüttl, T. J. and Friedrich, R., Low-Reynolds-number effects derived from direct numerical simulations of turbulent pipe flow, *Computer and fluids*, **30**, 2001, 581 – 590.

[26] Wu, X. and Moin, P., A direct numerical simulation study on the mean velocity characteristics in turbulent pipe flow, *Journal of Fluid Mechanics.*, **608**, 2008, 81 – 112.